Cannabinoids Inhibit Insulin Receptor Signaling in Pancreatic \(\beta\)-Cells

Cannabinoids Inhibit Insulin Receptor Signaling in Pancreatic β-Cells

Wook Kim,[1] Máire E. Doyle,[2] Zhuo Liu,[1] Qizong Lao,[1] Yu-Kyong Shin,[1] Olga D. Carlson,[1] Hee Seung Kim,[1] Sam Thomas,[1] Joshua K. Napora,[1] Eun Kyung Lee,[1] Ruin Moaddel,[1] Yan Wang,[1] Stuart Maudsley,[1] Bronwen Martin,[1] Rohit N. Kulkarni,[3] and Josephine M. Egan[1]

OBJECTIVE—Optimal glucose homeostasis requires exquisitely precise adaptation of the number of insulin-secreting β-cells in the islets of Langerhans. Insulin itself positively regulates β-cell proliferation in an autocrine manner through the insulin receptor (IR) signaling pathway. It is now coming to light that cannabinoid 1 receptor (CB1R) agonism/antagonism influences insulin action in insulin-sensitive tissues. However, the cells on which the CB1Rs are expressed and their function in islets have not been firmly established. We undertook the current study to investigate if intraislet endogenous cannabinoids (ECs) regulate β-cell proliferation and if they influence insulin action.

RESEARCH DESIGN AND METHODS—We measured EC production in isolated human and mouse islets and β-cell line in response to glucose and KCl. We evaluated human and mouse islets, several β-cell lines, and CB1R-null (*CB1R*$^{-/-}$) mice for the presence of a fully functioning EC system. We investigated if ECs influence β-cell physiology through regulating insulin action and demonstrated the therapeutic potential of manipulation of the EC system in diabetic (*db/db*) mice.

RESULTS—ECs are generated within β-cells, which also express CB1Rs that are fully functioning when activated by ligands. Genetic and pharmacologic blockade of CB1R results in enhanced IR signaling through the insulin receptor substrate 2-AKT pathway in β-cells and leads to increased β-cell proliferation and mass. CB1R antagonism in *db/db* mice results in reduced blood glucose and increased β-cell proliferation and mass, coupled with enhanced IR signaling in β-cells. Furthermore, CB1R activation impedes insulin-stimulated IR autophosphorylation on β-cells in a $G\alpha_i$-dependent manner.

CONCLUSIONS—These findings provide direct evidence for a functional interaction between CB1R and IR signaling involved in the regulation of β-cell proliferation and will serve as a basis for developing new therapeutic interventions to enhance β-cell function and proliferation in diabetes. ***Diabetes*** **60:1198–1209, 2011**

Insulin is the prime mediator of glucose homeostasis. A paucity (as occurs in type 1 diabetes) or surplus (due to excessive exogenous insulin administration or insulin-secreting tumors) of insulin causes somatic damage by energy deprivation and neuroglucopenic brain damage. Therefore, the number of insulin-secreting β-cells is tightly regulated to maintain a very narrow blood glucose range. Intriguingly, insulin also has major effects on its own secretory cells. Exogenously infused insulin increases β-cell mass (1), and mice lacking β-cell insulin receptors (IRs) develop insulin-dependent diabetes because of insufficient β-cell proliferation and defective insulin secretion (2,3). IR activation on β-cells, in addition to being necessary for optimal function of the glucose sensing machinery (3), causes phosphorylation of insulin receptor substrate 2 (IRS2), which then transduces the signal to the AKT-forkhead box protein O1 (FoxO1) cascade and increases β-cell proliferation (4).

The endogenous cannabinoids (ECs), 2-arachidonoylglycerol (2-AG), and anandamide (AEA), are lipid transmitters synthesized only on demand by Ca^{2+}-dependent enzymes in the brain and the periphery (5,6). The biologic effects of ECs are mediated by two G protein-coupled receptors (CB1R and CB2R) that use the $G\alpha_i$ class of heterotrimeric proteins to regulate intracellular signaling pathways (5). ECs are key players of feeding behavior through the activation of the CB1Rs in the brain (5). Initial studies found that CB1Rs are expressed mainly in the brain and modulate food intake and energy balance.

However, new evidence has accumulated that suggests that ECs also influence insulin action through peripheral CB1Rs in insulin-sensitive tissues, such as adipose tissue, liver, and muscle, and that these effects are independent of food intake or central CB1R activation (6). Indeed, AEA impairs insulin-stimulated AKT phosphorylation and decreases glucose uptake in skeletal muscle cells (7), and CB1R antagonism enhances insulin responsiveness of skeletal muscle (8). However, the mechanism by which CB1R regulates insulin action remains unknown.

Recent studies have extended this notion to the endocrine pancreas, where CB1Rs and EC metabolic enzymes were found in rodent and human islets (9–15). The cells on which CB1Rs are expressed have not been firmly established, however. Initial studies suggested that CB1Rs are densely located in α-cells and to a lesser degree in β-cells (10,11), another reported the absence of CB1R in β-cells (13), whereas still other reports point to the presence of CB1R in β-cells (9,12,14,15). The presence of CB2R in β-cells is also controversial. Studies reported the presence of CB2R in β-cells (9,11,15), whereas other studies pointed to the absence of CB2R in β-cells (10,12). Here, we tried to settle the controversy over the existence of the EC receptors in β-cells and provide a novel, fundamental, and potentially exploitable function for CB1Rs in insulin-mediated β-cell proliferation. We found that an intraislet EC system (ECS) indeed exists and serves as a negative feedback on insulin-mediated β-cell proliferation. We also

From the [1]National Institute on Aging, National Institutes of Health, Baltimore, Maryland; the [2]Division of Endocrinology, Johns Hopkins Medical Institutes, Baltimore, Maryland; and the [3]Department of Islet Cell Biology and Regenerative Medicine, Joslin Diabetes Center, and Department of Medicine, Harvard Medical School, Boston, Massachusetts.
Corresponding author: Josephine M. Egan, eganj@grc.nia.nih.gov.
Received 9 November 2010 and accepted 4 January 2011.
DOI: 10.2337/db10-1550
This article contains Supplementary Data online at http://diabetes.diabetesjournals.org/lookup/suppl/doi:10.2337/db10-1550/-/DC1.

demonstrate the therapeutic potential of manipulation of the ECS in a mouse model of type 2 diabetes.

RESEARCH DESIGN AND METHODS

Materials. Sources and dilutions of primary antibodies used in immunoblotting, immunoprecipitation, and immunostaining are listed in Supplementary Table 1. AEA, 2-AG, AEA-d8, 2-AG-d5, WIN55,212-2, arachidonyl-2-chloroethylamide (ACEA), AM251, and AM630 were obtained from Cayman Chemical (Ann Arbor, MI). GFP-HA-tagged CB1R was from K. Mackie (Indiana University). The human IR and $G\alpha_{i3}$ cDNA were amplified by RT-PCR from a human pancreas RNA (Stratagene, La Jolla, CA), with oligo-dT (18 bp) for the reverse transcription. The IR cDNA was incorporated into a 3×Flag vector and the $G\alpha_{i3}$ cDNA was incorporated into an mVenus-C1 vector. IR mutant (IR-3YA), whose Tyr1158/1162/1163 residues were substituted to Ala, was generated from wild-type IR (IR-WT) using a QuikChange II XL site-directed mutagenesis kit (Stratagene).

Animal experiments. $CB1R^{-/-}$ mice and their WT littermates were developed and backcrossed to a C57Bl/6 J background, as previously described (16). The study used male 2- to 3-month-old $CB1R^{+/+}$ and $CB1R^{-/-}$ mice. AM251 (10 mg/kg) was administrated by daily intraperitoneal injection to 1-month-old normal C57Bl/6 J mice for 4 weeks. $FAAH^{-/-}$ mice were obtained from Dr. Benjamin Cravatt (Scripps Research Institute), and 1-month-old *db/db* mice were from The Jackson Laboratory (Bar Harbor, ME).

DMSO, AM251 (10 mg/kg), and AM630 (10 mg/kg) were injected daily for 4 weeks. Then, the pancreata were dissected and blood was collected in the ad lib state of eating. Blood glucose concentration was measured using an Elite glucometer (Bayer Healthcare, Tarrytown NY), and plasma insulin was measured using a rat/mouse insulin ELISA Kit (Crystal Chem, Downers Grove, IL). All animal care and experimental procedures followed National Institutes of Health (NIH) guidelines and were approved by the National Institute on Aging Animal Care and Use Committee.

Immunostaining and pancreas morphometry. Pancreata were fixed in 4% paraformaldehyde, immersed in 20% sucrose before freezing, and sectioned (7-μm thickness). Human and mouse paraffin-embedded pancreatic sections were immunostained as before (17). After antigen unmasking, the slides were incubated with primary antibodies (Supplementary Table 1), followed by secondary antibodies (Invitrogen, Carlsbad, CA) along with TO-PRO-3 (Invitrogen), in some cases, for nuclear staining.

Slides were viewed using a LSM-710 confocal microscope (Carl Zeiss MicroImaging, München-Hallbergmoos, Germany). Multiple sections from 3 to 5 mice per group, separated by at least 200 μm from each section, were assessed for signal intensity and the number of nuclear p27- or proliferating cell nuclear antigen (PCNA)-positive ($PCNA^+$) β-cells with LSM Image Browser software (Carl Zeiss). To determine β-cell area and mass, the pancreata were trimmed of all nonpancreatic tissue and processed for immunostaining. The cross-sectional areas of pancreata and β-cells were determined from multiple sections (n = 5 mice per group), separated by at least 200 μm from each section, using LSM Image Browser software. The relative cross-sectional area of β-cells was determined by quantification of the cross-sectional area covered by insulin-positive cells divided by the cross-sectional area of total pancreas tissue. The β-cell mass per pancreas was estimated as the product of the relative cross-sectional area of β-cells per total tissue and the weight of the pancreas.

Islet isolation and EC levels. Human islets were provided by the Islet Cell Resource Center. Mouse islets were isolated using collagenase digestion, as we previously described (18). Human or mouse islets in Dulbecco's modified Eagle's medium (DMEM) containing 4 mmol/L glucose and 1% BSA were pelleted and incubated with DMEM containing 4, 10, or 15 mmol/L glucose, with or without KCl (30 mmol/L) for 10 min. Lipid extraction and tandem mass spectrometry analysis were done next, and details are described in the Supplementary Data.

Laser capture microdissection of β-cells. We used the PixCell II Workstation (Arcturus Engineering, Carlsbad, CA) to perform laser capture microdissection and image acquisition of β-cells in pancreas sections, as we previously described (17). Total RNAs were isolated using the PicoPure RNA Isolation Kit (Arcturus), according to the manufacturer's instructions. After reverse transcription, the resulting materials were used for quantitative (q)RT-PCR amplification using gene-specific primer pairs and SYBR Green PCR master mix (Applied Biosystems, Carlsbad, CA).

Cell culture, transfection, and proliferation studies. β-IRWT and β-IRKO cells were established from mice (2,19,20). β-IRWT, β-IRKO, MIN6, β-TC6, and α-TC1 cells were maintained in DMEM with 10% FBS (Invitrogen). CHO-K1 and CHO-IR (CHO-K1 cells stably transfected with IR) cells were maintained in DMEM/F-12 with 10% FBS. Human neuroblastoma BE(2)-M17 cells were maintained in OPTI-MEM with 10% FBS. Transfections of small interfering (si) RNAs (Santa Cruz Biotechnology, Santa Cruz, CA) for $G\alpha_{i3}$ and CB1R and the expression vectors for CB1R, $G\alpha_{i3}$, and IR were done using lipofectamine RNAiMAX or 2000 (Invitrogen). Scramble siRNA (Silencer Negative Control #1; Ambion, Austin, TX) or empty vector was transfected as the negative control. For exogenous insulin treatment, cells starved overnight in low-glucose DMEM containing 0.1% FBS were incubated for 2 h in glucose-free DMEM with 0.1% BSA, followed by pretreatment with CB1R agonists for 15 min and insulin stimulation for 10 min, with or without CB1R agonists. For cell proliferation studies, cells were plated into 96-well plates with complete medium. After treatment with CB1R antagonist or agonists, or both, the proliferation rate was determined after 48 or 72 h using the CellTiter 96 Aqueous One Solution Cell Proliferation Assay (Promega, Madison, WI), according to the manufacturer's instructions.

Immunoprecipitation and $G\alpha_i$ activation assay. Cell lysates extracted using radioimmunoprecipitation assay buffer (RIPA) containing protease and phosphatase inhibitor cocktails were incubated with the appropriate antibody and subsequently incubated with protein A/G beads. Beads were washed three times with RIPA buffer and underwent Western blot analysis with the primary antibodies and with an HRP-conjugated secondary antibody. Blots were visualized by enhanced chemiluminescence (GE Health, Berne, Switzerland). For $G\alpha_i$ activation assay, we used the $G\alpha_i$ Activation Assay Kit (NewEast Biosciences, Malvern, PA) as previously described (21). Cells treated with or without ACEA were lysed with ice-cold 1×Assay/Lysis buffer and underwent immunoprecipitation with anti-$G\alpha_i$–guanosine triphosphate (GTP) antibody and Western blot analysis with anti-$G\alpha_{i3}$ antibody. For positive control, β-IRWT cell lysate, not treated with ACEA, was incubated with guanosine 5'-O-[γ-thio] triphosphate (GTP-γS) for 90 min before immunoprecipitation.

Statistical analysis. Quantitative data are presented as the mean ± SEM. Differences between mean values were compared statistically by Student t test. Comparisons were performed by using GraphPad Prism (GraphPad Software, La Jolla, CA). A P value of < 0.05 was considered statistically significant.

RESULTS

Islets have a self-contained ECS. CB1Rs are present in β- and α-cells in both mouse (Fig. 1*A*) and human (Fig. 1*B*) islets. To confirm specificity of staining, we used pancreata from $CB1R^{-/-}$ mice (16) (Fig. 1*A*) and the corresponding blocking peptides (Fig. 1*A*). For added proof of our findings, we microdissected β-cells from islets of $CB1R^{+/+}$ and $CB1R^{-/-}$ mice by laser-capture microscopy, and using qRT-PCR of the captured cells, we confirmed *CB1R* expression (Fig. 1*C*). Western blot analysis showed that CB1Rs are expressed in mouse insulinoma (β-TC6 and MIN6) and glucagonoma (α-TC1) cells (Supplementary Fig. 1*A*). CB2Rs are absent in β- and α-cells, but cellular CB2R staining is evident in islets (Fig. 1*D*). Of general interest, and as previously reported (10), the CB2Rs are present in somatostatin-containing cells in islets (Fig. 1*E*).

Also as previously reported (11), EC-synthetic enzymes, *N*-acyl-phosphatidyl ethanolamine phospholipase D (NAPE-PLD; Fig. 2*A*) and diacylglycerol lipase-α (DAGLα) (Fig. 2*B*) are present mainly in β-cells, with little if any expression in α-cells in both human and mouse islets. The EC-degrading enzyme, fatty acid amide hydrolase (FAAH), is present mainly in β-cells (Fig. 2*C*), and monoacyl glycerol lipase (MAGL) is present in both β- and α-cells (Fig. 2*D*) in human and mouse islets. In agreement with published literature (9,10), increasing glucose concentrations increased 2-AG and AEA levels in human (Fig. 2*E*) and mouse (Fig. 2*F*) islets, and membrane depolarization with KCl also increased 2-AG and AEA levels in human islets (Fig. 2*E*). Consistently, glucose and KCl also increased 2-AG levels in insulin-secreting immortalized β-cells (β-IRWT) established from mice (2,19,20) (Supplementary Fig. 1*B*). Thus, these results favor the presence of an entire self-contained ECS in mouse and human islets.

Enhanced IR signaling and β-cell proliferation due to CB1R antagonism. The $CB1R^{-/-}$ mice are known to have a lean phenotype and are resistant to weight gain, even

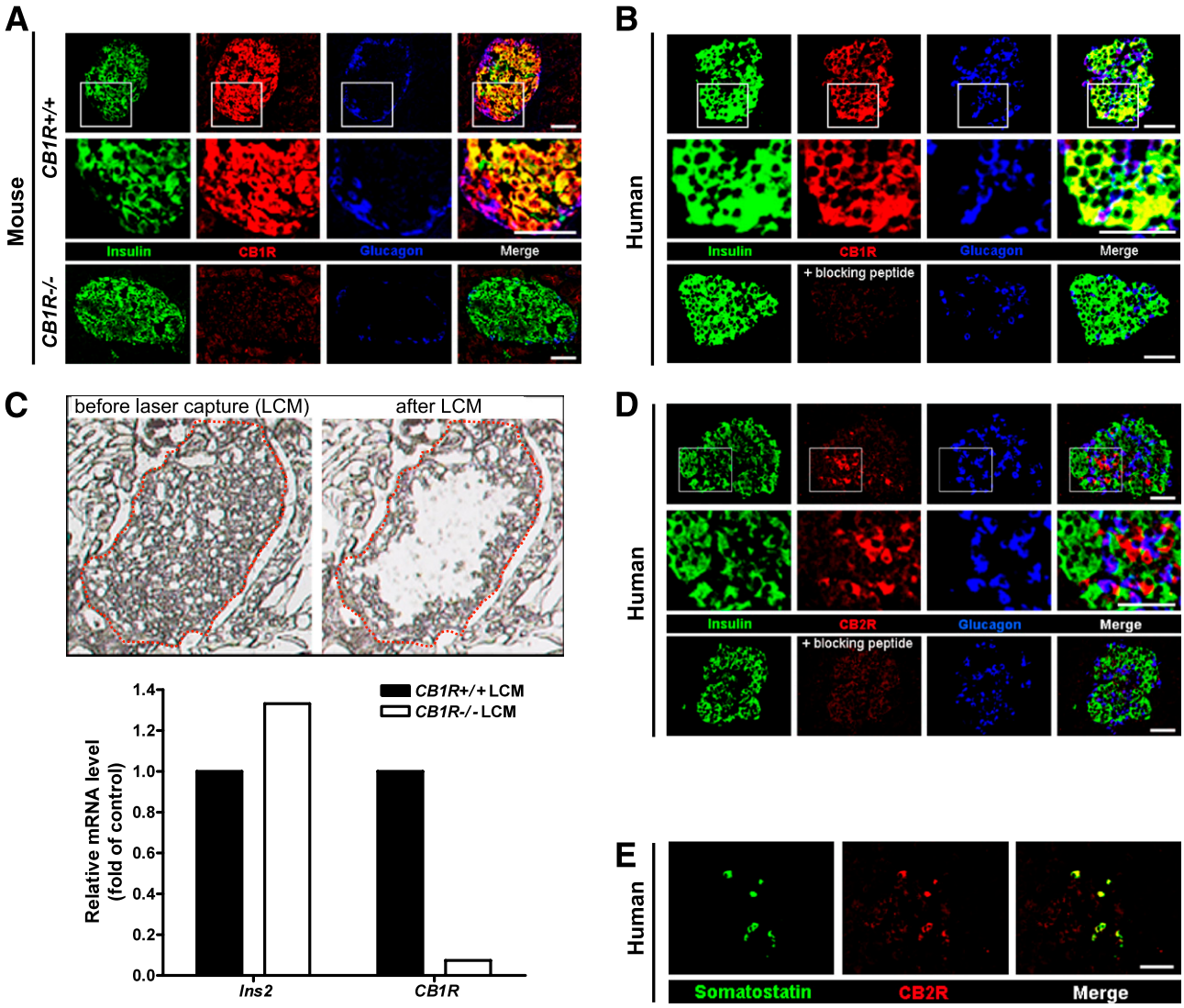

FIG. 1. The presence of CB1R in pancreatic β-cells. *A*: Immunostaining for CB1R in pancreatic sections from *CB1R*$^{+/+}$ and *CB1R*$^{-/-}$ mice. Boxed areas are magnified and shown on the *bottom panel*. Scale bar = 50 μm. *B*: Immunostaining for CB1R in human islets. The specificity of anti-CB1R antibody was assessed by antigen preabsorption with the corresponding blocking peptides. Boxed areas are magnified and shown on the *bottom panel*. Scale bar = 50 μm. *C*: qRT-PCR amplification of *insulin* (*ins2*) and *CB1R* mRNA from laser-captured β-cells of *CB1R*$^{+/+}$ and *CB1R*$^{-/-}$ mice. Data were normalized to *18S* levels. The *upper panel* shows a representative image of islets before and after laser capture of β-cells. *D*: Immunostaining for CB2R in human islets. The specificity of anti-CB2R antibody was assessed by antigen preabsorption with the corresponding blocking peptides. Boxed areas are magnified and shown on the *bottom panel*. Scale bar = 50 μm. *E*: Immunostaining for somatostatin and CB2R in human islets. Scale bar = 50 μm. (A high-quality digital representation of this figure is available in the online issue.)

when fed a high-fat diet, and to have improved glucose tolerance and insulin sensitivity compared with WT mice (22,23). Consistently, treatment with CB1R ligands leads to glucose intolerance and insulin resistance in rodents (23–25) and conversely, peripheral, but not central, CB1R antagonism caused weight-independent improvement in glucose tolerance, insulin sensitivity, fatty liver, and plasma lipid profile even in mice with genetic or diet-induced obesity (23,25,26). These effects are independent of food intake or central CB1R activation (6,23,26).

Their pancreata have not been previously studied. We found that the amount of phosphorylated IR at Y1162/1163 (*p*-IR), IRS1/2 at Y612 (*p*-IRS1/2), and AKT at S473 (*p*-AKT) were all higher in the islets of *CB1R*$^{-/-}$ mice compared with age-matched *CB1R*$^{+/+}$ mice (Fig. 3*A*). Because IR signaling is a key regulator of β-cell proliferation (1–4,27–29), we investigated β-cell area and islet size in *CB1R*$^{-/-}$ mice. In keeping with enhanced IR signaling in isolated islets of *CB1R*$^{-/-}$ mice, β-cell area (Fig. 3*B*) and islet size (Fig. 3*C*), but not pancreas wet weight of *CB1R*$^{+/+}$ (0.216 g ± 0.02 g) versus *CB1R*$^{-/-}$ (0.196 ± 0.02 g, n = 6 per genotype, P = 0.48), were increased, and the distribution of islet size (Fig. 3*D*) was shifted toward bigger islets in *CB1R*$^{-/-}$ compared with *CB1R*$^{+/+}$ mice. PCNA, a marker of cell proliferation, was more readily apparent in nuclei of β-cells in *CB1R*$^{-/-}$ mice than in *CB1R*$^{+/+}$ mice (Fig. 3*E*). Ki-67 staining, another marker of cell proliferation, generated similar results (data not shown). Concordant with these observations, CB1R blockade by AM251 also led to increases in β-cell area (Fig. 3*F*) and PCNA^{+} β-cells (Fig. 3*G*), compared with DMSO-treated animals.

CB1R blockade leads to increased β-cell mass in *db/db* mice. Genetic and pharmacologic blockade of CB1R in mice with diet-induced obesity results in improved

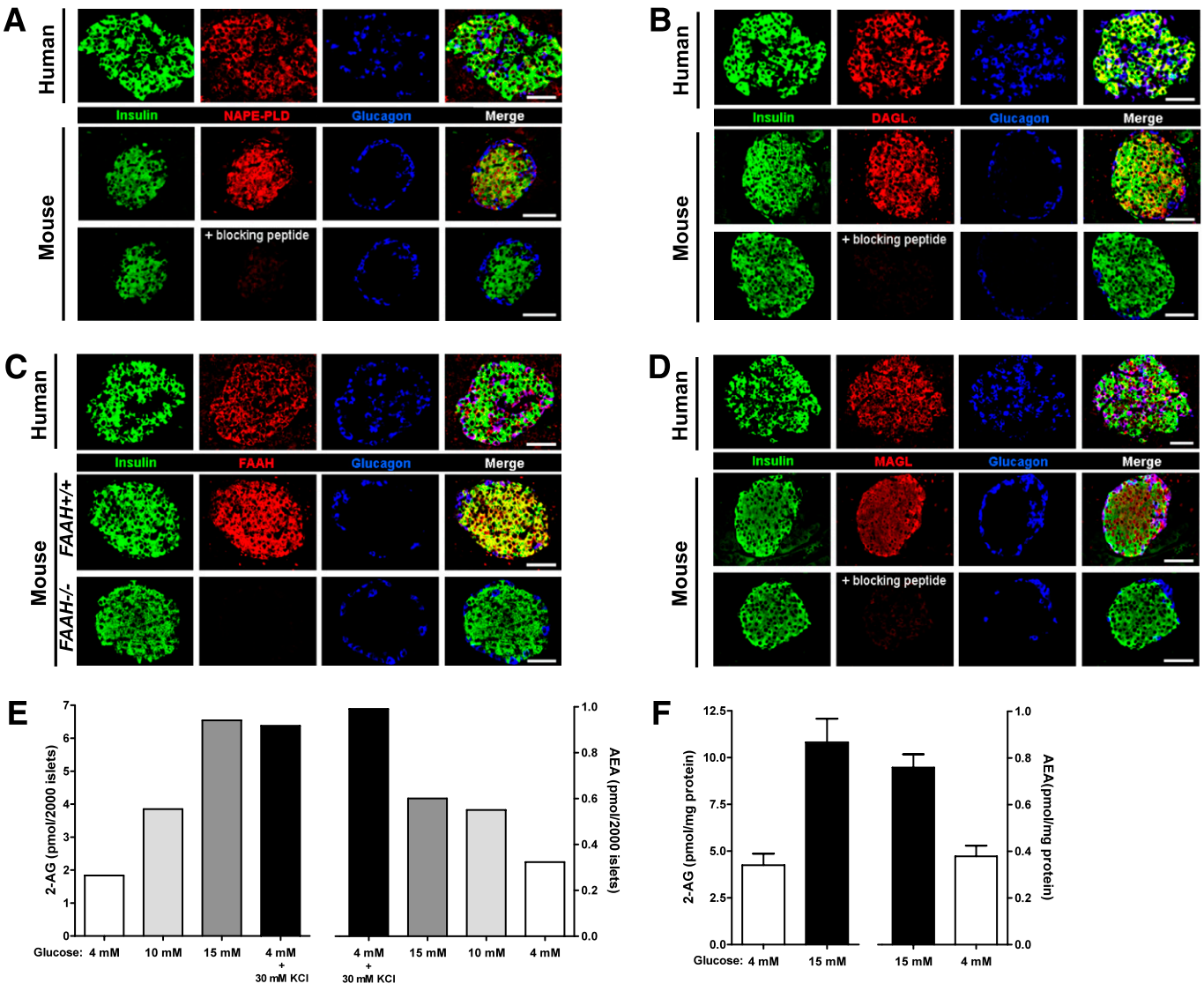

FIG. 2. Identification of intraislet ECS. *A* and *B*: Immunostaining for NAPE-PLD (*A*) and DAGLα (*B*) in human and mouse islets. The specificity of anti-NAPE-PLD and anti-DAGLα antibodies was assessed by antigen preabsorption with the corresponding blocking peptides. Scale bar = 50 μm. *C*: Immunostaining for FAAH in pancreatic sections of human and *FAAH*$^{+/+}$ and *FAAH*$^{-/-}$ mice. Scale bar = 50 μm. *D*: Immunostaining for MAGL in human and mouse islets. The specificity of anti-MAGL antibody was assessed by antigen preabsorption with the corresponding blocking peptides. Scale bar = 50 μm. *E*: Levels of AEA and 2-AG extracted from one lot of human islets exposed to the indicated glucose concentrations with or without KCl for 10 min. The amount of AEA and 2-AG in the samples were determined by calculating the ratio of abundance of AEA or 2-AG to the internal standard abundance. *F*: Levels of AEA and 2-AG extracted from mouse islets exposed to the indicated glucose concentrations for 10 min. The amount of AEA and 2-AG in the samples were determined by calculating the ratio of abundance of AEA or 2-AG to the internal standard abundance. Data are shown as the mean ± SEM from two independent experiments. (A high-quality digital representation of this figure is available in the online issue.)

glucose tolerance and insulin sensitivity (23,25,26,30). Because genetic CB1R ablation resulted in larger islets and enhanced β-cell proliferation, despite improved insulin sensitivity, we investigated if CB1R modulation would be beneficial to β-cells in a mouse model of type 2 diabetes. We injected DMSO, AM251, or AM630 (a CB2R antagonist) daily into 4-week-old *db/db* mice for 4 weeks (Fig. 4*A*). Consistent with previous reports (23,25,26,30), AM251-treated mice had lower body weight (Fig. 4*B*) and blood glucose (Fig. 4*C*) and plasma insulin (Fig. 4*D*) levels than DMSO-treated mice, whereas AM630 had no obvious effects (Fig. 4*B–D*). Pancreatic sections showed increased intraislet insulin content and total β-cell mass in AM251-treated mice compared with DMSO-treated mice (Fig. 4*E–G*), which was most likely due to enhanced β-cell proliferation (Fig. 4*H*).

Given that AKT regulates p27^{Kip1} (p27) activity, an inhibitor of cell cycle progression, by affecting its abundance and subcellular localization (31,32), and that accumulation of p27 in the nuclei of β-cells contributes to deficient β-cell mass and proliferation during the development of type 2 diabetes in *Irs2*$^{-/-}$ and *db/db* mice (28), we examined the expression and subcellular localization of p27. Immunostaining of pancreatic sections from AM251-treated mice showed a significant decrease in the total amount and nuclear localization of p27 in β-cells, with most of the protein being localized in cytoplasm, compared with DMSO-treated mice (Fig. 4*I*). To evaluate whether the

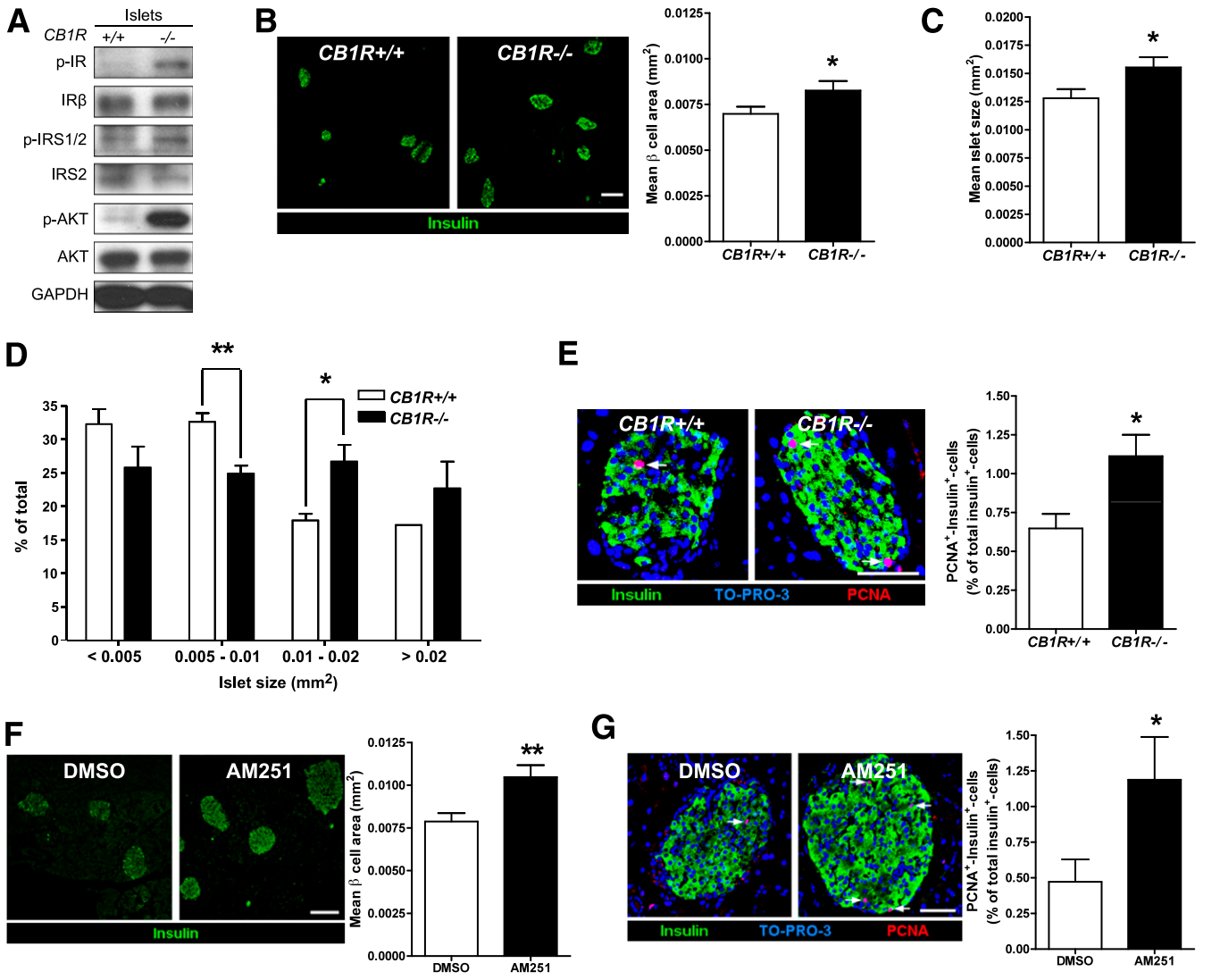

FIG. 3. Effects of CB1R antagonism on β-cell proliferation. *A*: Western blot analysis for the indicated proteins in isolated islets from overnight-fasted *CB1R*$^{+/+}$ and *CB1R*$^{-/-}$ mice. Glyceraldehyde-3-phosphate dehydrogenase (GAPDH) was used as a loading control. *B*: Representative immunostaining for insulin in *CB1R*$^{+/+}$ and *CB1R*$^{-/-}$ mice. Scale bar = 200 μm. Mean β-cell area is shown on the *right*. *C* and *D*: Mean islet size (*C*) and islet size distribution (*D*) of *CB1R*$^{+/+}$ and *CB1R*$^{-/-}$ mice. The data were estimated from at least 225 islets per genotype. *E*: Pancreatic sections of cohorts in *panel B*, showing PCNA$^+$ β-cells as indicated by arrows. Scale bar = 50 μm. Quantification of PCNA$^+$ β-cells is shown on the *right*. The number of cells that are positive for both PCNA and insulin were quantified as a percentage of the total number of insulin-positive cells in the sections. *F*: Representative immunostaining for insulin in DMSO- and AM251-injected mice. Scale bar = 200 μm. Mean β-cell area of DMSO- and AM251-treated mice is shown on the *right*. *G*: Pancreatic sections of cohorts in *F*, showing PCNA$^+$ β-cells as indicated by arrows. Scale bar = 50 μm. Quantification of PCNA$^+$ β-cells is shown on the *right*. The number of cells that are positive for both PCNA and insulin were quantified as a percentage of the total number of insulin-positive cells in the sections. Data are shown as the mean ± SEM in all panels (*n* = 3–5 animals per group). **P* < 0.05; ***P* < 0.01. (A high-quality digital representation of this figure is available in the online issue.)

increased β-cell proliferation seen by CB1R antagonism associates with any changes in IR signaling, we examined phosphorylation levels of IR. The amount of *p*-IR was significantly increased in AM251-treated mice compared with DMSO-treated mice (Fig. 4*G*).

CB1R inhibits β-cell proliferation by impeding IR autophosphorylation. Because pharmacologic and genetic blockade of CB1Rs led to enhanced IR signaling and β-cell proliferation, we next investigated the potential role of IRs as a/the mediator of CB1R-controlled β-cell proliferation. We used β-cells established from control (β-IRWT) and β-cell–specific IR knockout (β-IRKO) mice (2,19,20) in which expression levels of CB1Rs are similar (Fig. 5*A*). The selective synthetic CB1R agonist ACEA slowed proliferation of β-IRWT cells that was prevented by AM251 (Fig. 5*B*).

As previously reported (19), β-IRKO cells already had significantly reduced proliferation rates compared with β-IRWT cells (Fig. 5*C*). The proliferation rate of β-IRWT was increased by AM251 (Fig. 5*D*) and decreased by ACEA (Fig. 5*E*), whereas both compounds had no or a lesser effect on β-IRKO cells (Fig. 5*D* and *E*). Consistently, ACEA dose-dependently decreased levels of *p*-IRS1/2, *p*-AKT, and *p*-FoxO1 (Fig. 5*F*) and increased p27 expression (Fig. 5*A*) in β-IRWT cells, but not in β-IRKO cells. CB1R blockade by AM251 in normal mice also resulted in a significant decrease in both the amount and nuclear localization of p27 (Fig. 5*G*) compared with DMSO-treated animals. These results suggest that CB1R signaling functions as a negative regulator of the proliferative effects of endogenously secreted insulin from β-cells.

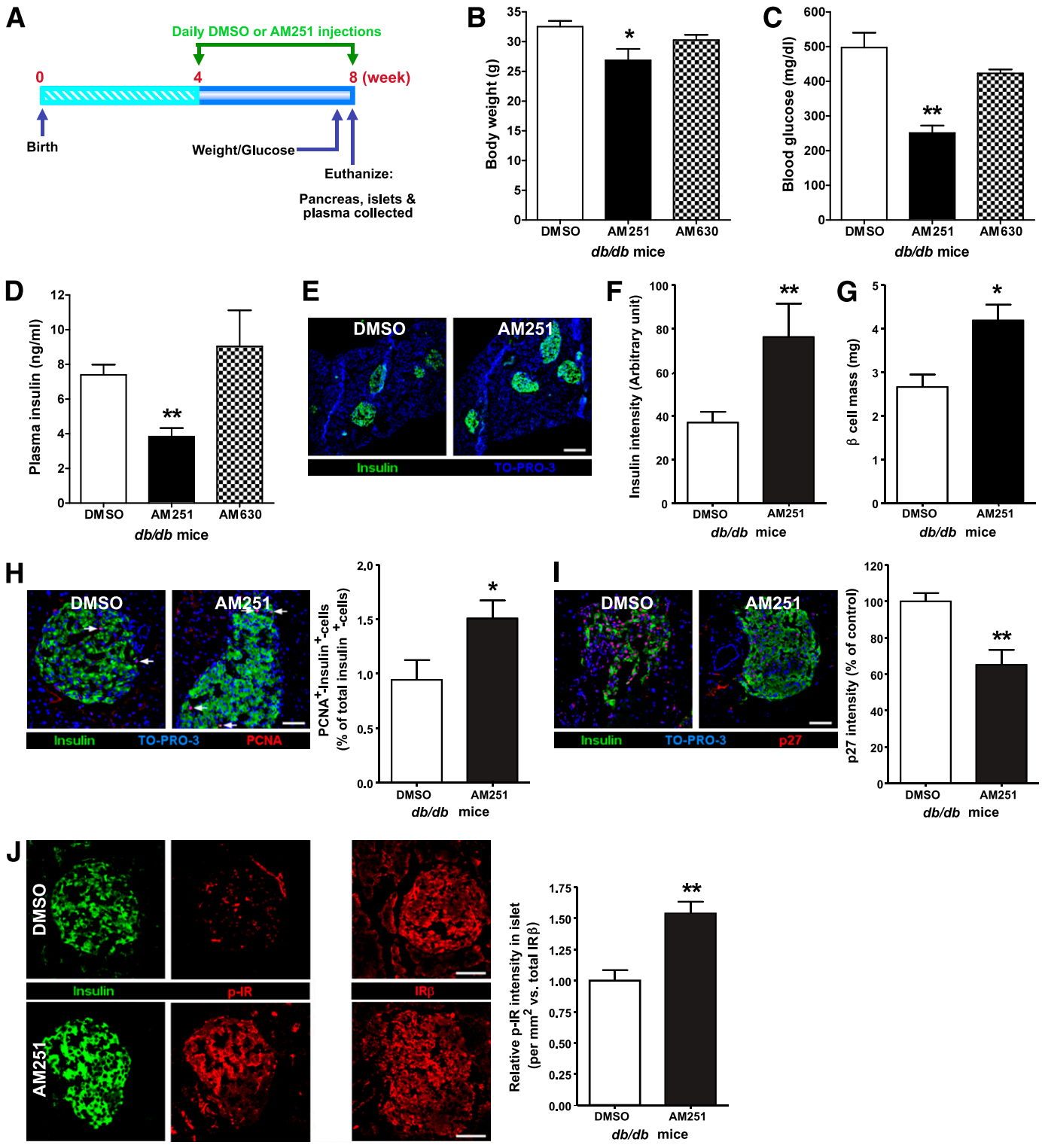

FIG. 4. Increased β-cell mass and proliferation in AM251-treated *db/db* mice. *A*: Experimental timeline for DMSO, AM251, or AM630 (CB2R antagonist) treatment in 4-week-old *db/db* mice. DMSO, AM251 (10 mg/kg), or AM630 (10 mg/kg), were administrated by daily intraperitoneal injection for 4 weeks. *B*: Body weight of DMSO-, AM251-, or AM630-treated *db/db* mice. *C* and *D*: Blood glucose (*C*) and plasma insulin (*D*) levels at the end of the 4-week period. *E*: Representative images for insulin in *db/db* mice injected with DMSO or AM251 for 4 weeks. Scale bar = 200 μm. *F*: Quantification of insulin intensity in islets of cohorts in *E*. *G*: Morphometric assessment of β-cell mass of cohorts in *E*. *H*: Representative images of PCNA$^+$ β-cells in islets of cohorts in *E*. Arrows denote PCNA$^+$ β-cells. Scale bar = 50 μm. Quantification of PCNA$^+$ β-cells is shown on the right. The number of cells that are positive for both PCNA and insulin were quantified as a percentage of the total number of insulin-positive cells in the sections. *I*: Representative immunostaining for insulin and p27 in islets of cohorts in *E*. Scale bar = 50 μm. Relative signal intensity for p27 in islet is shown on the *right*. *J*: Representative immunostaining for IR and *p*-IR in islets of cohorts in *E*. Scale bar = 50 μm. Relative signal intensity for *p*-IR in islets is shown on the *right*. Intensity for *p*-IR was normalized to that for total IR-β. Data are shown as the mean ± SEM in all panels (n = 5 animals per group). *$P < 0.05$; **$P < 0.01$. (A high-quality digital representation of this figure is available in the online issue.)

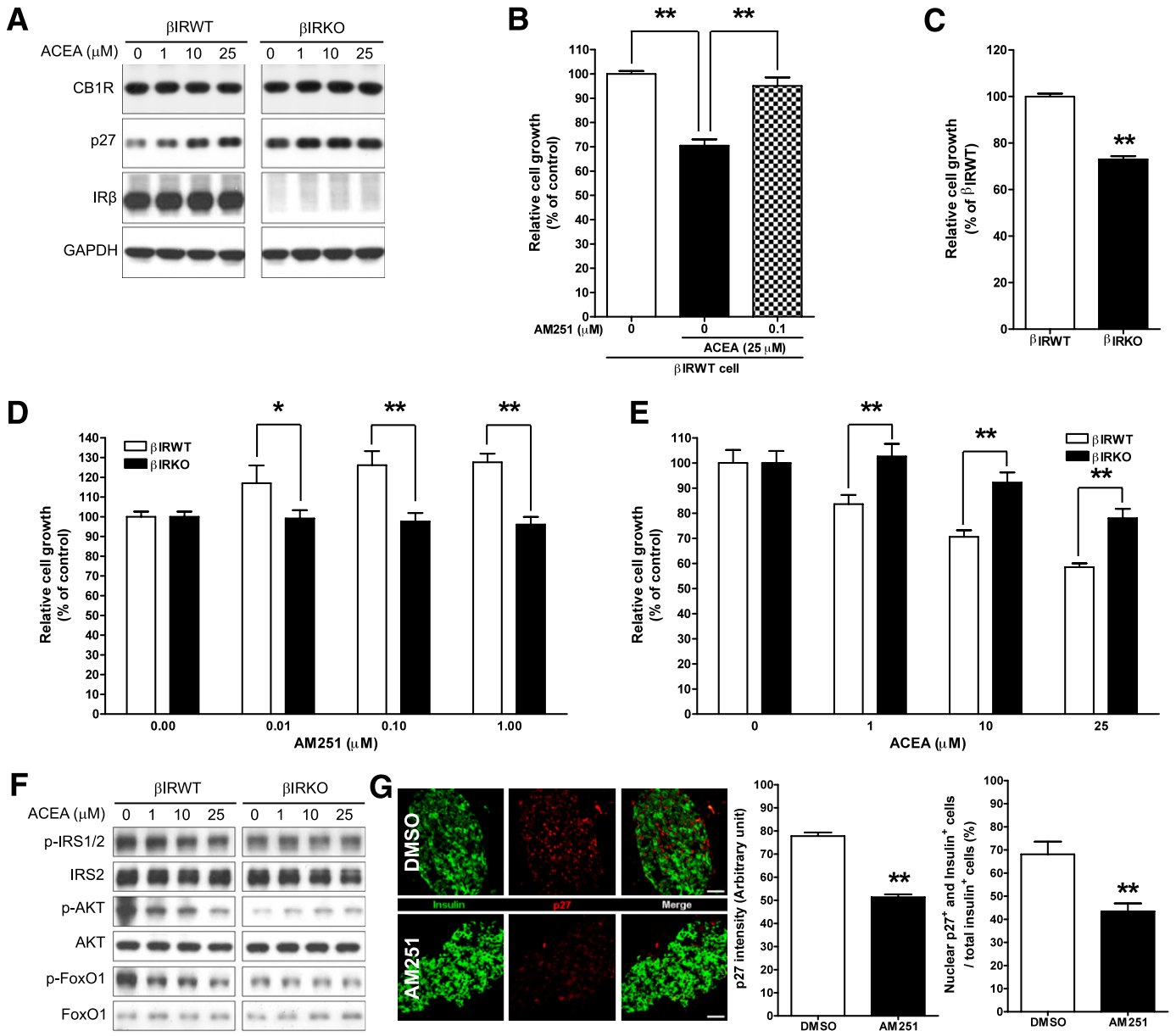

FIG. 5. Inhibitory effects of CB1R on β-cell proliferation depends on IR. *A*: Levels of CB1R, p27, and IR in β-IRWT and β-IRKO cells exposed to a selective synthetic CB1R agonist ACEA for 40 h. *B*: Proliferation rates of β-IRWT cells exposed to ACEA with or without AM251 for 48 h. Data are shown as the mean ± SEM from three independent experiments. **$P < 0.01$. *C*: Proliferation rates of β-IRWT and β-IRKO cells 3 days after plating. Data are shown as the mean ± SEM from three independent experiments. **$P < 0.01$. *D*: Effects of AM251 on the proliferation of β-IRWT and β-IRKO cells. Data are shown as the mean ± SEM from three independent experiments. *$P < 0.05$; **$P < 0.01$. *E*: Effects of ACEA (48 h) on the proliferation of β-IRWT and β-IRKO cells. Data are shown as the mean ± SEM from three independent experiments. **$P < 0.01$. *F*: Levels of the indicated proteins in β-IRWT and β-IRKO cells exposed to ACEA for 40 h. *G*: Representative immunostaining of insulin and p27 in pancreatic sections from DMSO- and AM251-injected mice. Scale bar = 50 μm. Quantification of p27 intensity and nuclear p27$^+$ β-cells in islets is shown on the *bottom*. Data are shown as the mean ± SEM ($n = 3$ per group). **$P < 0.01$. (A high-quality digital representation of this figure is available in the online issue.)

To test the direct effect of CB1R activation on IR activity, isolated mouse islets (Fig. 6*A*) and β-IRWT cells (Fig. 6*B*) were pretreated with AEA or 2-AG and ACEA, respectively, before addition of exogenous insulin. All agonists markedly prevented exogenous insulin-stimulated IR autophosphorylation and downstream signaling. This was also true in BE(2)-M17 human neuroblastoma cells (data not shown), which express CB1Rs (Supplementary Fig. 1*A*). In addition, ACEA diminished exogenous insulin-stimulated IR autophosphorylation and levels of *p*-IRS1/2, *p*-PDK1, *p*-AKT, and *p*-FoxO1 in MIN6 cells (data not shown). The inhibitory effects of CB1R agonists on IR autophosphorylation and *p*-AKT were not observed in CHO cells (CHO cells lack CB1Rs, see Supplementary Fig. 1*A*; Fig. 6*C*), but ACEA treatment in CHO-IR (CHO cells stably transfected with IR) cells transfected with the expression vector containing GFP-HA–tagged CB1R led to reduced IR autophosphorylation (Fig. 6*D*).

To directly confirm the inhibitory effects of CB1R on IR autophosphorylation, we transfected Flag-tagged IR-WT and IR mutant (IR-3YA), whose Tyr1158/1162/1163 residues were substituted to Ala (Fig. 6*E*), into β-IRKO cells and then treated the cells with ACEA for 40 h (Fig. 6*F*). IR autophosphorylation was detected in IR-WT–transfected β-IRKO cells, presumably due to endogenous insulin secretion, and ACEA reduced levels of *p*-IR and *p*-AKT in

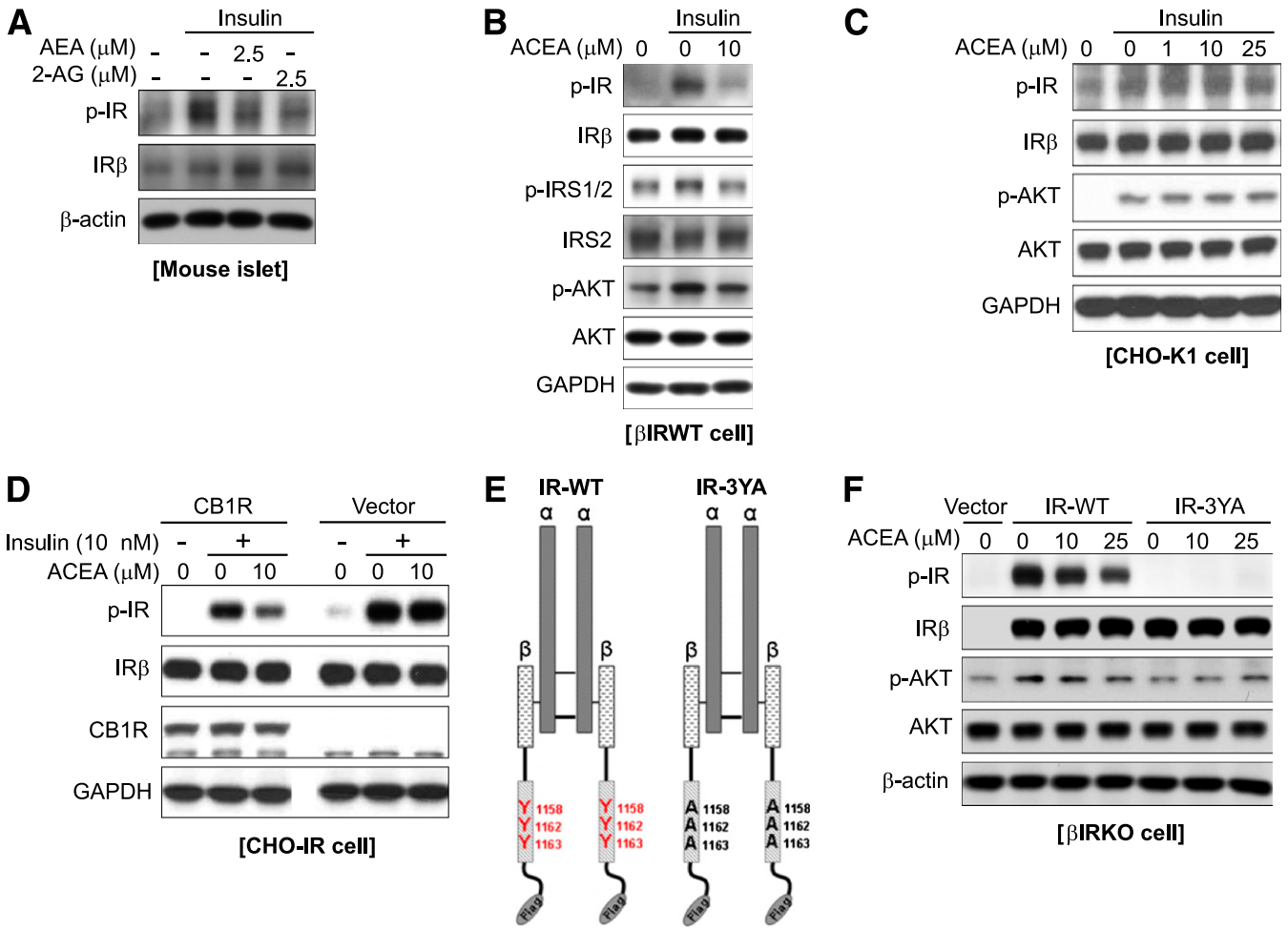

FIG. 6. Regulation of IR activity by CB1R. ***A*****: Phosphorylation levels of *p*-IR in isolated mouse islets exposed to insulin (10 nmol/L) for 10 min with vehicle, AEA or 2-AG.** ***B*****: Western blot analysis of the indicated proteins in β-IRWT cells exposed to insulin (10 min) with ACEA or vehicle.** ***C*****: Levels of *p*-IR and *p*-AKT in CHO-K1 cells exposed to insulin with or without ACEA.** ***D*****: Effects of CB1R over-expression on insulin-stimulated IR autophosphorylation. CHO-IR cells transiently transfected with the indicated plasmids were preincubated with ACEA for 20 min before insulin treatment (10 min), after which their lysates were subjected to Western blot analysis for the indicated proteins.** ***E*****: Substitution of IR autophosphorylation sites (Tyr1158/1162/1163) with Ala.** ***F*****: Western blot analysis for the indicated proteins in β-IRKO cells exposed to ACEA for 40 h after transfection with empty vector, IR-WT, or IR-3YA. (A high-quality color representation of this figure is available in the online issue.)**

those cells, but in IR-3YA–transfected β-IRKO cells, *p*-AKT levels were not altered (Fig. 6*F*). In sum, these results suggest a functional interaction between CB1R and IR signaling upon IR autophosphorylation.

Inhibitory effect of CB1R on IR signaling depends on Gα_i. Activated CB1Rs mediate their intracellular actions through Gα_i proteins (5). Gα_{i3} appears to be expressed mainly in β-cells of both human and mouse (Fig. 7*A*), and its activity was increased by CB1R activation in both β-IRWT and β-IRKO cells (Fig. 7*B*). ACEA dose-dependently increased the association between Gα_{i3} and IR (Fig. 7*C*), whereas siRNA-mediated attenuation of CB1Rs (Supplementary Fig. 2*A*) reduced the association (Fig. 7*C*). Furthermore, exogenous insulin treatment led to a decrease in Gα_{i3}/IR association, which was impeded by ACEA (Fig. 7*D*).

We further confirmed an EC-mediated Gα_{i3}/IR association using IR-WT and IR-3YA–transfected β-IRKO cells with or without ACEA treatment for 15 min. As shown in Fig. 6*E*, ACEA reduced levels of *p*-IR and *p*-AKT in IR-WT–transfected β-IRKO cells, but *p*-AKT was not reduced in IR-3YA–transfected β-IRKO cells (Fig. 7*E*), and most interestingly, Gα_{i3} association with IR-3YA was actually increased compared with IR-WT (Fig. 7*F* and *G*). ACEA increased Gα_{i3}/IR association (Fig. 7*F*), which conversely was reduced by AM251 (Fig. 7*G*). These results suggest that Gα_i mediates the inhibitory effect of CB1R activation on IR autophosphorylation by its association with IR. Furthermore, over-expression of Gα_{i3} in β-IRWT cells led to decreased levels of *p*-IR and *p*-IRS1/2 (Fig. 8*A*) and knockdown of CB1Rs (Supplementary Fig. 2*A*) or Gα_{i3} (Supplementary Fig. 2*B*) by siRNA in β-IRWT cells abolished the ability of ACEA to inhibit insulin-stimulated phosphorylation of IR, IRS1/2, and AKT (Fig. 8*B*) as well as its ability to increase p27 expression (Fig. 8*C*). Consistently, knockdown of CB1Rs or Gα_{i3} resulted in an increase in β-cell proliferation (Fig. 8*D*) and a loss of the inhibitory actions of ACEA (Fig. 8*E*). These results suggest that the CB1R-mediated effects on IR and downstream signaling involve EC-induced activation of Gα_i.

DISCUSSION

In contrast to adipose tissue, liver, and muscle, the presence and effects of CB1Rs in β-cells have been inconclusive. Here, we demonstrate that β-cells contain all of the components of a self-contained ECS: CB1R, the

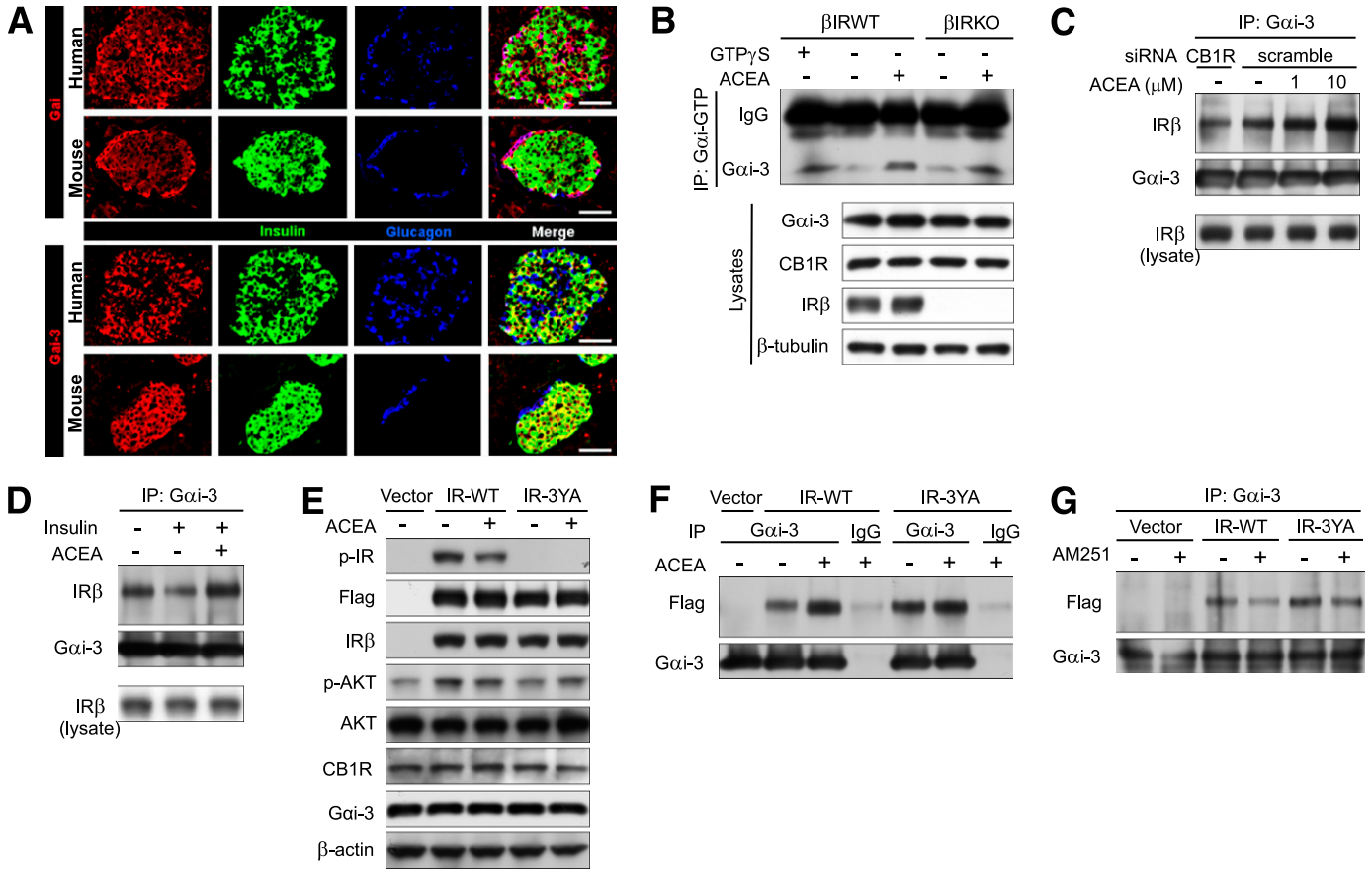

FIG. 7. Activation of CB1Rs increases the association between $G\alpha_{i3}$ and IR. *A*: Immunostaining for $G\alpha_i$ and $G\alpha_{i3}$ in human and mouse islets. Anti-$G\alpha_i$ antibody recognizes $G\alpha_{i1}$, $G\alpha_{i2}$, and $G\alpha_{i3}$. Scale bar = 50 μm. *B*: $G\alpha_i$ activation assay in β-IRWT and β-IRKO cells. Lysates of β-IRWT and β-IRKO cells treated with or without ACEA (10 μmol/L) for 20 min were subjected to immunoprecipitation with anti-$G\alpha_i$-GTP and to immunoblotting with anti-$G\alpha_{i3}$. For positive control, β-IRWT cell lysate not treated with ACEA was incubated with GTP-γS for 90 min before immunoprecipitation. *C*: Endogenous $G\alpha_{i3}$/IR interaction in β-IRWT cells exposed to ACEA or vehicle (15 min) after transfection of the indicated siRNAs. *D*: Endogenous $G\alpha_{i3}$/IR interaction in β-IRWT cells exposed to insulin (10 nmol/L) with or without ACEA (10 μmol/L). *E*: Western blot analysis for the indicated proteins in β-IRKO cells exposed to ACEA (10 μmol/L) for 15 min after transfection with empty vector, IR-WT, or IR-3YA. *F*: Increase of $G\alpha_{i3}$/IR interaction by ACEA in β-IRKO cells of cohorts in *E*. *G*: Reduction of $G\alpha_{i3}$/IR interaction by AM251 in β-IRKO cells transfected with empty vector, IR-WT, or IR-3YA. (A high-quality digital representation of this figure is available in the online issue.)

necessary enzymes for catalyzing EC biosynthesis and degradation, and the capacity to generate ECs in response to glucose stimulation and depolarization, even when isolated from the pancreas. We used several antibodies (33,34), including the L15 antibody to the C-terminus of CB1R that exhibits the expression pattern most consistent with in-situ hybridization (33) as well as qRT-PCR of laser-captured β-cells from islets, to affirm that CB1Rs, but not CB2Rs, are present on β-cells of mice and men. Bermúdez-Silva et al. (14) have very recently written that using the L15 antibody they also found a CB1R signal with insulin costaining; after using a commercially available CB1R antibody, they reported that CB1Rs were mainly expressed in α-cells (10). CB2Rs are absent from α- and β-cells. Most reports, including this study, found that β-cells contain EC synthetic and degrading enzymes (9–11,14).

Since at least 1979, insulin mediators, also referred to as insulin second messengers, are known to be generated from lipid precursors present on plasma membranes in response to IR activation and consequent downstream phospholipase activation (35). We are now suggesting that ECs, also generated from lipid precursors in β-cells, influence IR activation (Supplementary Fig. 3). This is especially relevant because insulin concentrations would be expected to be at their highest levels surrounding β-cells and therefore the islet ECS potentially evolved to prevent an over-exuberant β-cell IR signaling cascade. Favoring this view are our findings that in various β-cell lines, isolated islets and a mouse model of diabetes CB1R signaling counteracts the effects of insulin on β-cells by preventing IR autophosphorylation and downstream signals. This finding was not unique to pancreatic β-cells because activation of CB1Rs also impeded exogenous insulin-stimulated IR autophosphorylation in non-insulin-secreting cells.

We also found that $G\alpha_i$, which is involved in the regulation of insulin secretion (36) and β-cell proliferation (37), mediates the inhibitory effect of CB1R activation on IR activity by its association with IR. CB1R activation increased $G\alpha_{i3}$ activity and $G\alpha_{i3}$/IR association was strengthened by CB1R activation and substitution of Tyr1158/1162/1163 residues of IR with Ala, which, conversely, was weakened by suppression of CB1R activity and by insulin. Furthermore, knockdown of $G\alpha_{i3}$ by siRNA abolished the ability of CB1R to inhibit exogenous insulin-stimulated IR autophosphorylation and β-cell proliferation.

These results suggest a functional and physical crosstalk between CB1R and IR signaling upon IR autophosphorylation in a $G\alpha_i$-dependent manner. Given that binding of insulin to the extracellular α-chains of IR causes a change

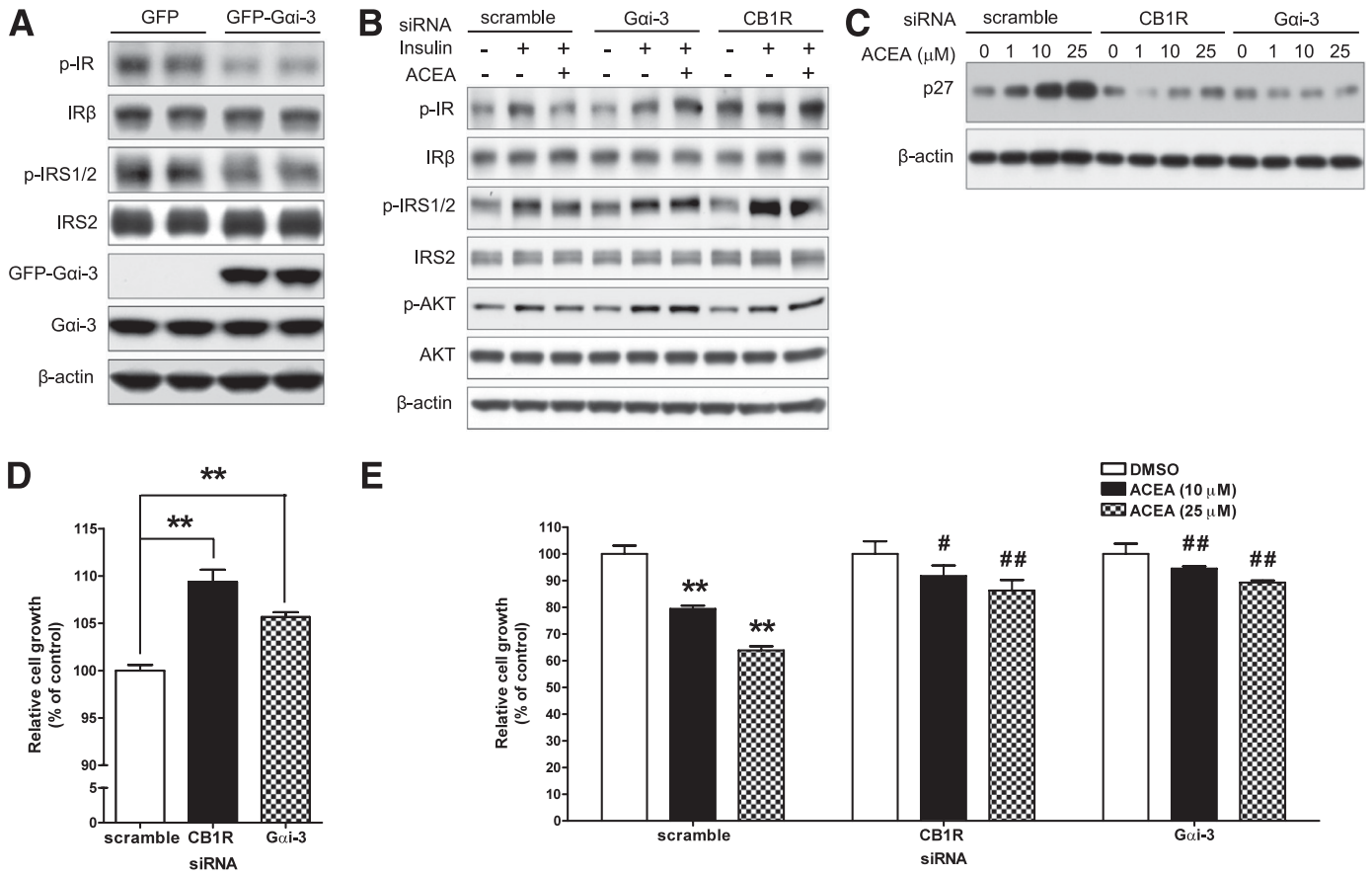

FIG. 8. Inhibitory effects of CB1R on IR signaling require $G\alpha_i$. *A*: Effects of $G\alpha_{i3}$ over-expression on *p*-IR and *p*-IRS1/2 in β-IRWT cells. *B*: Phosphorylation of IR, IRS1/2, and AKT in β-IRWT cells exposed to insulin (10 nmol/L) with ACEA (10 μmol/L) or vehicle after transfection of the indicated siRNAs. *C*: Level of p27 in β-IRWT cells exposed to ACEA for 40 h after transfection of the indicated siRNAs. *D*: Comparison of the proliferation rate between β-IRWT cells transfected with scramble, CB1R, or $G\alpha_{i3}$ siRNA. The relative proliferation rate of β-IRWT cells was determined 3 days after transfection. Data are shown as the mean ± SEM from three independent experiments. **$P < 0.01$. *E*: Effects of ACEA on the proliferation of β-IRWT cells transfected with the indicated siRNAs. Data are shown as the mean ± SEM from three independent experiments. **$P < 0.01$ vs. vehicle; #$P < 0.05$; ##$P < 0.01$ vs. scramble siRNA.

within the quaternary structure of IR that places the phosphorylation sites of one β-chain within reach of the active site of the other β-chain and that results in autophosphorylation at Tyr1158/1162/1163 residues in the activation loop of the β-chains (38,39), we propose that $G\alpha_{i3}$ activated by CB1R associates with unphosphorylated IR at the Tyr1158/1162/1163 residues, preventing a conformational change that secures the activation loop in a catalytically competent configuration upon ligand binding.

Because these receptors are found to be present within caveolae, a cholesterol-rich microdomain that performs a number of signaling functions (40), it is possible that the closeness of the CB1Rs causes them to be involved in modulating IR-mediated signaling. Although the detailed molecular mechanism underlying CB1R and $G\alpha_{i3}$ as regulatory components in the IR signaling pathway awaits further exploration, collectively, our results imply that the alteration in IR activity by CB1Rs is a reflection of a direct inhibition of IR autophosphorylation in a $G\alpha_i$-dependent manner and that ECs directly regulate proliferation through activation of CB1Rs expressed in β-cells. Through these actions, CB1Rs are likely to set a threshold level for IR-mediated responses, which depends on the level of expression or activation of CB1R. Alteration in IR activity by CB1Rs may additionally be due to the change in autocrine activation because of altered insulin secretion. CB1R-mediated suppression of insulin secretion in a Ca^{2+}-dependent manner has been reported (12,41); however, there are also reports to the contrary (9,10,15,42,43).

We demonstrate the therapeutic advantage of CB1R modulation in a type 2 diabetic condition. Inhibition of CB1R activity in *db/db* mice led to reduced blood glucose and increased β-cell proliferation, coupled with enhanced IR signaling. There is also evidence that insulin itself reduces glucose-stimulated EC synthesis in β-cells, which would serve as a negative feedback loop to reduce intraislet EC levels (9). This would logically mean that when IR function is reduced, as in type 2 diabetes, such a robust feedback would also be impaired, leading to nonphysiologic EC levels in islets (in addition to in fat and liver) and consequent CB1R-mediated β-cell dysfunction through further impeding IR activity. Blocking CB1Rs would therefore be expected to improve β-cell function in *db/db* mice, as we found. CB2R antagonism had no such effects.

An inadequate expansion of β-cell mass or failure of the existing β-cell mass to compensate for the changing insulin demand are hallmarks of type 2 diabetes, and these prominent features may result from defective IR signaling (1–4,27–29). Therefore, our data should result in the resumption of attention being paid to ECS as a key factor in β-cell physiology and may lead to development of a new therapeutic strategy aiming to preserve better functioning β-cells.

EC levels, not only in the circulating blood but also in the pancreas, are said to be elevated in diabetes and obesity (9,11,44,45), and elevated EC levels are associated with increased DAGLα and decreased FAAH levels in β-cells (11). Thus, it is possible that increased EC tone (due to increased EC synthesis, receptor expression or activity) affects the well-described glucose-unresponsiveness of β-cells and the development of insulin resistance by impeding IR autophosphorylation in insulin-sensitive tissues. Indeed, AEA was recently found to impair insulin-stimulated AKT phosphorylation and decrease glucose uptake in skeletal muscle cells (7), and CB1R antagonism enhanced insulin responsiveness of skeletal muscle (8).

In addition, pharmacologic blockade of CB1R in obese *fa/fa* Zucker rats decreased blood glucose levels and preserved β-cell mass (46), and eliminating CB1Rs in liver protected against fatty liver and improved glucose tolerance and insulin sensitivity in high-fat diet–fed mice (23); IR function in those mice was not investigated. Peripheral, but not central, blockade of CB1R was recently reported to improve overall insulin sensitivity and glucose homeostasis (26) and a non-brain-penetrant CB1R antagonist improved glucose homeostasis, insulin sensitivity, and fatty liver in a weight-independent manner (25). This is a very important point, because a centrally acting CB1R antagonist, rimonabant, used for treating obesity, was removed from patient use because of potentially life-threatening psychiatric problems (47). Therefore, CB1R antagonists with poor brain penetrance might be useful therapies in type 2 diabetes where they would be expected to lessen insulin resistance in skeletal muscle and liver, ameliorate or prevent fatty liver, and improve β-cell function/proliferation.

ACKNOWLEDGMENTS

This work was supported by the Intramural Research Program of the National Institute on Aging (NIA)/NIH. R.N.K. is supported by NIH R01-DK-67536 and 68721. M.E.D. is supported by JDRF 26-2008-864.

No potential conflicts of interest relevant to this article were reported.

W.K. designed and performed experiments, contributed to discussion, and wrote, reviewed, and edited the manuscript. M.E.D. designed and performed some experiments and provided advice and reagents. Z.L. performed some experiments and analyzed data. Q.L. designed and performed some experiments and provided advice and reagents. Y.-K.S., O.D.C., and H.S.K. performed some experiments and analyzed data. S.T. and J.K.N. analyzed data. E.K.L. contributed to the design of some experiments, the interpretation of data, and discussion. R.M. and Y.W. performed some experiments and analyzed data. S.M. and B.M. contributed to the design of some experiments, the interpretation of data, and discussion. R.N.K. provided advice and reagents and contributed to the interpretation of data and discussion. J.M.E. designed and performed experiments, contributed to the interpretation of data, and wrote, reviewed, and edited the manuscript.

The authors thank Dr. K. Mackie (Indiana University) for specific CB1R (L15 antibody, in particular) and DAGLα antibodies, and for the expression vector containing GFP-HA-tagged rat *CB1R* cDNA, and Dr. Benjamin Cravatt (Scripps Research Institute) for providing *FAAH*$^{-/-}$ mice. The authors are grateful to the staff of the Bioanalytical Chemistry Section/NIA (chief, Dr. I. Wainer) for developing the methodology for quantifying ECs in islets, to the staff in the Confocal Microscopy Unit/NIA (chief, Dr. F. Indig), and to the Histology Core/NIA (Dr. M. Xu, in particular). Dr. J. Pickel, NIMH Transgenic Core/NIH, provided the *CB1R*$^{-/-}$ mice and the animal facilities of NIA/NIH and carried out the genotyping and husbandry. The authors thank Dr. R. Broch (NIA/NIH) for discussions of technical procedures and manuscript readings. The ongoing support and encouragement of our Scientific Director, Dr. D. Longo, were vital for all stages of this work.

REFERENCES

1. Paris M, Bernard-Kargar C, Berthault MF, Bouwens L, Ktorza A. Specific and combined effects of insulin and glucose on functional pancreatic beta-cell mass in vivo in adult rats. Endocrinology 2003;144:2717–2727
2. Kulkarni RN, Brüning JC, Winnay JN, Postic C, Magnuson MA, Kahn CR. Tissue-specific knockout of the insulin receptor in pancreatic beta cells creates an insulin secretory defect similar to that in type 2 diabetes. Cell 1999;96:329–339
3. Otani K, Kulkarni RN, Baldwin AC, et al. Reduced beta-cell mass and altered glucose sensing impair insulin-secretory function in betaIRKO mice. Am J Physiol Endocrinol Metab 2004;286:E41–E49
4. Withers DJ, Gutierrez JS, Towery H, et al. Disruption of IRS-2 causes type 2 diabetes in mice. Nature 1998;391:900–904
5. Pagotto U, Marsicano G, Cota D, Lutz B, Pasquali R. The emerging role of the endocannabinoid system in endocrine regulation and energy balance. Endocr Rev 2006;27:73–100
6. Nogueiras R, Diaz-Arteaga A, Lockie SH, et al. The endocannabinoid system: role in glucose and energy metabolism. Pharmacol Res 2009;60:93–98
7. Eckardt K, Sell H, Taube A, et al. Cannabinoid type 1 receptors in human skeletal muscle cells participate in the negative crosstalk between fat and muscle. Diabetologia 2009;52:664–674
8. Lipina C, Stretton C, Hastings S, et al. Regulation of MAP kinase-directed mitogenic and protein kinase B-mediated signaling by cannabinoid receptor type 1 in skeletal muscle cells. Diabetes 2010;59:375–385
9. Matias I, Gonthier MP, Orlando P, et al. Regulation, function, and dysregulation of endocannabinoids in models of adipose and beta-pancreatic cells and in obesity and hyperglycemia. J Clin Endocrinol Metab 2006;91:3171–3180
10. Bermúdez-Silva FJ, Suárez J, Baixeras E, et al. Presence of functional cannabinoid receptors in human endocrine pancreas. Diabetologia 2008;51:476–487
11. Starowicz KM, Cristino L, Matias I, et al. Endocannabinoid dysregulation in the pancreas and adipose tissue of mice fed with a high-fat diet. Obesity (Silver Spring) 2008;16:553–565
12. Nakata M, Yada T. Cannabinoids inhibit insulin secretion and cytosolic Ca^{2+} oscillation in islet β-cells via CB1 receptors. Regul Pept 2008;145:49–53
13. Tharp WG, Lee YH, Maple RL, Pratley RE. The cannabinoid CB1 receptor is expressed in pancreatic delta-cells. Biochem Biophys Res Commun 2008;372:595–600
14. Bermúdez-Silva FJ, Suárez Pérez J, Nadal A, Rodríguez de Fonseca F. The role of the pancreatic endocannabinoid system in glucose metabolism. Best Pract Res Clin Endocrinol Metab 2009;23:87–102
15. Li C, Jones PM, Persaud SJ. Cannabinoid receptors are coupled to stimulation of insulin secretion from mouse MIN6 beta-cells. Cell Physiol Biochem 2010;26:187–196
16. Zimmer A, Zimmer AM, Hohmann AG, Herkenham M, Bonner TI. Increased mortality, hypoactivity, and hypoalgesia in cannabinoid CB1 receptor knockout mice. Proc Natl Acad Sci U S A 1999;96:5780–5785
17. Theodorakis MJ, Carlson O, Michopoulos S, et al. Human duodenal enteroendocrine cells: source of both incretin peptides, GLP-1 and GIP. Am J Physiol Endocrinol Metab 2006;290:E550–E559
18. Perfetti R, Rafizadeh CM, Liotta AS, Egan JM. Age-dependent reduction in insulin secretion and insulin mRNA in isolated islets from rats. Am J Physiol 1995;269:E983–E990
19. Assmann A, Ueki K, Winnay JN, Kadowaki T, Kulkarni RN. Glucose effects on beta-cell growth and survival require activation of insulin receptors and insulin receptor substrate 2. Mol Cell Biol 2009;29:3219–3228
20. Kulkarni RN, Winnay JN, Daniels M, et al. Altered function of insulin receptor substrate-1-deficient mouse islets and cultured beta-cell lines. J Clin Invest 1999;104:R69–R75
21. Rajagopal S, Kim J, Ahn S, et al. Beta-arrestin- but not G protein-mediated signaling by the "decoy" receptor CXCR7. Proc Natl Acad Sci U S A 2010;107:628–632

22. Cota D, Marsicano G, Tschöp M, et al. The endogenous cannabinoid system affects energy balance via central orexigenic drive and peripheral lipogenesis. J Clin Invest 2003;112:423–431
23. Osei-Hyiaman D, Liu J, Zhou L, et al. Hepatic CB1 receptor is required for development of diet-induced steatosis, dyslipidemia, and insulin and leptin resistance in mice. J Clin Invest 2008;118:3160–3169
24. Bermúdez-Siva FJ, Serrano A, Diaz-Molina FJ, et al. Activation of cannabinoid CB1 receptors induces glucose intolerance in rats. Eur J Pharmacol 2006;531:282–284
25. Tam J, Vemuri VK, Liu J, et al. Peripheral CB1 cannabinoid receptor blockade improves cardiometabolic risk in mouse models of obesity. J Clin Invest 2010;120:2953–2966
26. Nogueiras R, Veyrat-Durebex C, Suchanek PM, et al. Peripheral, but not central, CB1 antagonism provides food intake-independent metabolic benefits in diet-induced obese rats. Diabetes 2008;57:2977–2991
27. Kitamura T, Nakae J, Kitamura Y, et al. The forkhead transcription factor Foxo1 links insulin signaling to Pdx1 regulation of pancreatic β cell growth. J Clin Invest 2002;110:1839–1847
28. Uchida T, Nakamura T, Hashimoto N, et al. Deletion of Cdkn1b ameliorates hyperglycemia by maintaining compensatory hyperinsulinemia in diabetic mice. Nat Med 2005;11:175–182
29. Hashimoto N, Kido Y, Uchida T, et al. Ablation of PDK1 in pancreatic beta cells induces diabetes as a result of loss of beta cell mass. Nat Genet 2006;38:589–593
30. Irwin N, Hunter K, Frizzell N, Flatt PR. Antidiabetic effects of sub-chronic administration of the cannabinoid receptor (CB1) antagonist, AM251, in obese diabetic (ob/ob) mice. Eur J Pharmacol 2008;581:226–233
31. Medema RH, Kops GJ, Bos JL, Burgering BM. AFX-like Forkhead transcription factors mediate cell-cycle regulation by Ras and PKB through p27kip1. Nature 2000;404:782–787
32. Cunningham MA, Zhu Q, Hammond JM. FoxO1a can alter cell cycle progression by regulating the nuclear localization of p27kip in granulosa cells. Mol Endocrinol 2004;18:1756–1767
33. Berghuis P, Rajnicek AM, Morozov YM, et al. Hardwiring the brain: endocannabinoids shape neuronal connectivity. Science 2007;316:1212–1216
34. Uchigashima M, Narushima M, Fukaya M, Katona I, Kano M, Watanabe M. Subcellular arrangement of molecules for 2-arachidonoyl-glycerol-mediated retrograde signaling and its physiological contribution to synaptic modulation in the striatum. J Neurosci 2007;27:3663–3676
35. Larner J, Galasko G, Cheng K, et al. Generation by insulin of a chemical mediator that controls protein phosphorylation and dephosphorylation. Science 1979;206:1408–1410
36. Regard JB, Kataoka H, Cano DA, et al. Probing cell type-specific functions of Gi in vivo identifies GPCR regulators of insulin secretion. J Clin Invest 2007;117:4034–4043
37. Kim H, Toyofuku Y, Lynn FC, et al. Serotonin regulates pancreatic beta cell mass during pregnancy. Nat Med 2010;16:804–808
38. Hubbard SR, Wei L, Ellis L, Hendrickson WA. Crystal structure of the tyrosine kinase domain of the human insulin receptor. Nature 1994;372:746–754
39. Hubbard SR. Juxtamembrane autoinhibition in receptor tyrosine kinases. Nat Rev Mol Cell Biol 2004;5:464–471
40. Sarnataro D, Grimaldi C, Pisanti S, et al. Plasma membrane and lysosomal localization of CB1 cannabinoid receptor are dependent on lipid rafts and regulated by anandamide in human breast cancer cells. FEBS Lett 2005;579:6343–6349
41. Juan-Picó P, Fuentes E, Bermúdez-Silva FJ, et al. Cannabinoid receptors regulate $Ca(^{2+})$ signals and insulin secretion in pancreatic β-cell. Cell Calcium 2006;39:155–162
42. Getty-Kaushik L, Richard AM, Deeney JT, Krawczyk S, Shirihai O, Corkey BE. The CB1 antagonist rimonabant decreases insulin hypersecretion in rat pancreatic islets. Obesity (Silver Spring) 2009;17:1856–1860
43. De Petrocellis L, Marini P, Matias I, et al. Mechanisms for the coupling of cannabinoid receptors to intracellular calcium mobilization in rat insulinoma beta-cells. Exp Cell Res 2007;313:2993–3004
44. Di Marzo V, Goparaju SK, Wang L, et al. Leptin-regulated endocannabinoids are involved in maintaining food intake. Nature 2001;410:822–825
45. Izzo AA, Piscitelli F, Capasso R, et al. Peripheral endocannabinoid dysregulation in obesity: relation to intestinal motility and energy processing induced by food deprivation and re-feeding. Br J Pharmacol 2009;158:451–461
46. Janiak P, Poirier B, Bidouard JP, et al. Blockade of cannabinoid CB1 receptors improves renal function, metabolic profile, and increased survival of obese Zucker rats. Kidney Int 2007;72:1345–1357
47. Akbas F, Gasteyger C, Sjödin A, Astrup A, Larsen TM. A critical review of the cannabinoid receptor as a drug target for obesity management. Obes Rev 2009;10:58–67